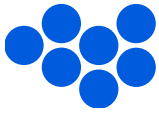

Bergen Center for Computational Science

BCCS

TECHNICAL REPORT SERIES

A 60 day hindcast study of the Norwegian Seas with focus on Ormen Lange using 20km and 4 km resolution

Helge Avlesen and Jarle Berntsen

REPORT No. 10 **June 2004**

UNIFOB

the University of Bergen research company

BERGEN, NORWAY

BCCS Technical Report Series is available at http://www.bccs.no/publications/

Requests for paper copies of this report can be sent to:

Bergen Center for Computational Science, Høyteknologisenteret,
Thormøhlensgate 55, N-5008 Bergen, Norway

A 60 day hindcast study of the Norwegian Seas with focus on Ormen Lange using 20km and 4 km resolution *

Helge Avlesen† and Jarle Berntsen‡

Computational Math Unit
Bergen Center for Computational Science
Thormøhlensgate 55
N-5008 Bergen
Norway

June 2004

Abstract

This report describes the setup and results from experiments using a σ-coordinate model with 20km and 4km resolution and slightly different extents of the Norwegian Seas. The models were forced with hindcast wind data from December 2002 and January 2003, while initial and boundary conditions were taken from climatology. The results show that the 4 kilometer model exhibits a vastly more dynamic and realistic behavior than both the 20km model and the reduced area 4km model. We found three factors to be very important in order to achieve realism with the numerical model. Using a larger domain enables the model to capture important remote large scale effects. Reduced viscosity improves the dynamic response to events in the forcing. Starting the simulation with a realistic stratification dramatically improves the results compared to starting from climatology.

1 Introduction

Ormen Lange (OL) is an offshore gas field located in the Storegga region off mid-Norway in water depths from approximately 800 to 1100m. The field, presently being developed under the leadership of Norsk Hydro, is located in the core of the Storegga slide that left an almost 300km long headwall at the shelf break. Extracting and transporting gas from the reservoir also involves seabed pipelines which makes it essential to know the maximum velocities in the region.

A data acquisition program at Ormen Lange (OL) has identified several events in which the currents close to the seabed and the rest of the water column exhibit short peak values in their speed, along with a peak in temperature. Thus, operating seabed installations needed for exploitation of the gas field may require precautions. It is therefore essential to understand the generation mechanisms behind these events and to investigate the possibility of forecasting them. An extensive program has been underway for a few years, with analysis of data from measurements as well as numerical modeling, applied to a large range of

*This work has been supported by Norsk Hydro under contract number 5259646
†Para//ab, BCCS, UNIFOB, University of Bergen. Email: avle@ii.uib.no
‡Department of Mathematics, University of Bergen. Email: jarleb@mi.uib.no

scales and phenomena. See reports by Eldevik, Eliassen, Berntsen, Furnes and Vikebø ([4], [2], [5], [3] and [14]) for more background information.

Mean temporal circulation at OL is strongly dominated by the Norwegian Atlantic Current. Tidal effects are weak. The extreme events seem to be driven by strong pressure gradients [15]. That is, strong atmospheric low pressures and/or internal pressure fronts between warmer Atlantic Water (AW) and colder Norwegian Sea Water (NSW). Along the shelf slope at OL, we may get steepening of the iso surfaces of density, separating AW and NSW, due to strong Ekman veering during storms or approaching internal density fronts. During such events, the density surfaces tend to undershoot their equilibrium level, and as the forcing weakens, the suppressed water may run up along the shelf slope. In this run up phase, peak values in the velocities are often found.

In this report, we present the setup and some results from experiments using three model setup's for the Norwegian Seas. One 4km resolution study was done with a limited area model. It eventually became clear that the conditions around Ormen Lange could be heavily influenced by large scale processes taking place outside the domain. Including such effects can be done in several ways, e.g., by feeding results from the 20km model into the reduced area model using a nesting technique, or by simply extending the 4km domain to include relevant areas. We chose the latter in order to not only get the effect of a larger domain atmospheric forcing, but also better resolved internal processes in the Atlantic inflow.

One of the length scales of processes related to internal pressure is the internal Rossby radius. In the Norwegian Seas this length scale is of the order 10-20 km. A rule of thumb says that approximately 10 grid points per wave length are necessary to resolve (or represent) a physical feature. This tells us that in a simulation with a resolution of 20km, such processes may not be resolved at all, while at 4km resolution we should start seeing the effects. So in a future study, even higher resolution is desirable, but the computational cost is currently, even with state of the art supercomputers, too high for research purposes.

Since the atmospheric forcing is believed to be a major forcing mechanism behind the observed events, we have studied the time series of a hindcast simulation in the water columns at station TH7 and TH8 of the measurement program, using forcing data from December 2002 and January 2003. The Norwegian Seas experienced some very strong low pressure systems in this period. The cross section passing through stations TH7 and TH8 is marked with a line in Figure 4. TH7 (label A in the figure) is located at approximately 400m depth while TH8 (label B) is located at ca. 860m depth. We observe that the magnitude of the depth, even in the 4km resolution model, can vary with 100m from one grid point to the next in the steep area around TH7 and TH8.

2 The numerical model

2.1 General setup and choice of parameters

Three basin scale models were set up, with climatological initial and boundary conditions described later. All models are variants of the Bergen Ocean Model (BOM), a 3D general circulation model for the ocean, developed by the Institute of Marine Research, the Department of Mathematics and the Department of Informatics at the University of Bergen. The code is publicly available and can be downloaded from the Internet at `http://www.mi.uib.no/BOM/`. The system of equations and the numerical model are described by [1]. The equations are the continuity equation for an incompressible fluid, the Reynolds averaged momentum equations horizontally, conservation equations for temperature and salinity, and the UNESCO-equation of state, see Gill [8]. The model assumes the Boussinesq and hydrostatic approximations. The equations are solved for 7 unknown 3D fields in the σ-coordinate system, where σ is a terrain-following coordinate representing the "vertical" z-direction. The unknowns are the horizontal velocities in the

x,y and σ-directions respectively: $U(x,y,z,t)$, $V(x,y,z,t)$ and $W(x,y,z,t)$, the salinity $S(x,y,z,t)$, the temperature $T(x,y,z,t)$, the turbulent length scales $Q2L(x,y,z,t)$ and $Q2(x,y,z,t)$ for the turbulence model, and one 2D field; the water elevation $\eta(x,y,t)$.

The first model with 20km resolution uses version 2 of BOM as the core. The second experiment uses the same model core, but with 4km resolution and covers a smaller area, just large enough to include the Ormen Lange area and a small fraction of the Atlantic inflow. The third model has 4km resolution, covers most of the Norwegian Seas, and was set up with version 4 of BOM. This version incorporates many new features, among them a new high order predictor corrector time stepping scheme that makes it possible to get stable solutions using smaller maximum viscosities in the solution of the momentum equations. When the resolution is increased, as in our case from 20km to 4km, this is quite important, since the numerical viscosity is proportional to the square of the resolution, and hence will be much smaller in magnitude for the high resolution experiments. The new time stepping scheme also makes it possible to march forward in time using longer time steps than in previous versions.

Equation 1 shows how the horizontal diffusivities A_M and A_H are computed, following Smagorinsky [13]:

$$(A_M, A_H) = (C_M, C_H)\Delta x\ \Delta y\ [(\frac{\partial U}{\partial x})^2 + \frac{1}{2}\ (\frac{\partial V}{\partial x} + \frac{\partial U}{\partial y})^2 + (\frac{\partial V}{\partial y})^2]^{\frac{1}{2}}, \qquad (1)$$

where Δx, Δy are the horizontal resolution in x and y directions respectively, and U, V the 3D horizontal velocities. Values for the constants C_M and C_H for the different runs performed are given in Table 1. Horizontal viscosities/diffusivity's that are too large may

Experiment	Model	C_M	C_{M2D}	C_H
A	20km, std. init. clim.	0.5	0.5	0
B	20km, std. init. clim.	0.1	0.1	0
C	20km, 20m thick isotherm	0.1	0.1	0
D	4km, small area	5	25	0
E	4km	0.2	0.2	0

Table 1: Parameters for the Smagorinsky turbulence closure scheme.

lead to numerical instabilities. We therefore enforce a maximum limit for A_M formulated as $A_{Mlimit} = 0.03125\Delta x^2/\Delta t$. In the large domain 4km resolution model, the C_M coefficients were multiplied by a factor of 10 in an area partly covering Great Britain (the rectangle with lower left coordinate 0,0 and upper right coordinate 200,300 in Figure 3) in order to avoid instabilities due to the very strong tides in this area. BOM has no flooding/drying of cells, so the model may fail when the surface elevation gets very close to, or hits the bottom. For the same reason, the minimum depth of the bathymetry is set to 10m in all experiments. In the same model, the values for C_M were multiplied with a factor of 100 inside the FRS zones to achieve the effect of the so-called Sponge layers, a well known technique used to avoid instabilities near open boundaries in other ocean models (POM, ROMS, MITgcm). The horizontal diffusivities are set to zero, to avoid artificial mixing along σ-layers. To obtain sharp fronts, a second order accurate TVD scheme is implemented for the advection terms of the momentum and transport equations, following Yang and Przekwas [16].

The vertical viscosities and diffusivities are modeled using the Mellor and Yamada [11] 2 1/2 level model. The governing equations include the modifications due to Galperin et al. [7] and are solved for turbulent kinetic energy, $q^2/2$, and turbulent macro scale, l, from which the vertical eddy viscosities and diffusivities are computed by way of empirical expressions. The vertical viscosity K_M is modified in a similar manner to the horizontal viscosity near the boundaries. A minimum value of $0.001m^2/s$ is enforced in the FRS zone.

The 20 km resolution model use 31 σ-layers in the vertical, while the 4km resolution models uses 41 σ-layers for the big domain and 46 layers for the small domain. In all models the layers are distributed according to Lynch et al. [9]. Their formula distributes the layers symmetrically around the mean depth, such that a gradually finer resolution towards the surface and the bottom is obtained after specifying only the desired σ-layer thickness of the bottom layer. The algorithm is quite simple and can be written like this

```
DELTAEPS = 1.0/(KB-1.)
PI = 4.*ATAN(1.0)
AA = (DELTAEPS - DSBOT)/SIN(2.*PI*DELTAEPS)
DO K = 1,KB
  EPS = (K-1.)/(KB-1.)
  Z(KB + 1 - K) = -1. + EPS - AA*SIN(2*PI*EPS)
END DO
```

Here `KB` is the number of layers, `DSBOT` is the desired bottom layer thickness and the σ-layers are returned in `Z`. Figure 1 shows the distribution of layers and layer thickness for each experiment. The models were run for 60 days, the large 4km model with an internal

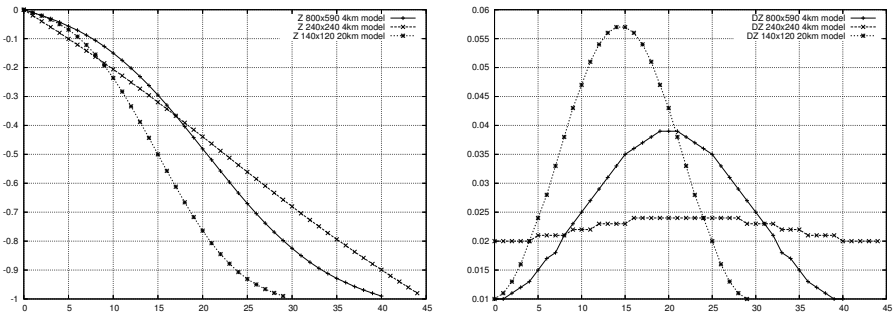

Figure 1: The vertical distribution of σ-layers for the three models. The left Figure shows σ-level versus point number, the right shows σ-layer thickness versus point number.

3-D time step of 260s and 40 2-D time steps per 3-D step, the small 4km model with an internal 3-D time step of 120s and 30 2-D time steps per 3-D step, the 20km model with an internal time step of 600 seconds and 30 2-D time steps per 3-D step.

2.2 Initial conditions and forcing

The initial values of water elevation, velocity, temperature and salinity used in all models are interpolated from the diagnostic climatology described in Engedahl [6].

At the lateral open boundaries, except at the boundary to the Baltic, a flow relaxation scheme (FRS) is implemented [10]. The FRS-zones are 7 cells wide for the 20km resolution model, and 10 grid cells wide for the 4km models. Climatological values of velocity, temperature, salinity and water elevation in addition to four tidal constituents (M_2, S_2, K_1, N_2) are used to specify the lateral boundary conditions in all three models. The models are also set up with fresh water run off from 27 rivers. However, these are disabled in the 4km models because we span only a 60 day period and have focus on the Ormen Lange area.

The 20km and 4km bathymetries are both based on data provided by the the Norwegian Meteorological Institute (met.no). In the area around Ormen Lange the bathymetry in the 4km resolution models was recovered from topographical data with up to 5m resolution provided by Norsk Hydro. Figure 4 shows the Ormen Lange area, and the new topographic features introduced by the high resolution data. In all models, the topography is smoothed slightly by applying a Shapiro Filter to the data.

All models were run in hindcast mode and forced using atmospheric pressure and wind provided by met.no. The hindcast wind and atmospheric pressure are from the months

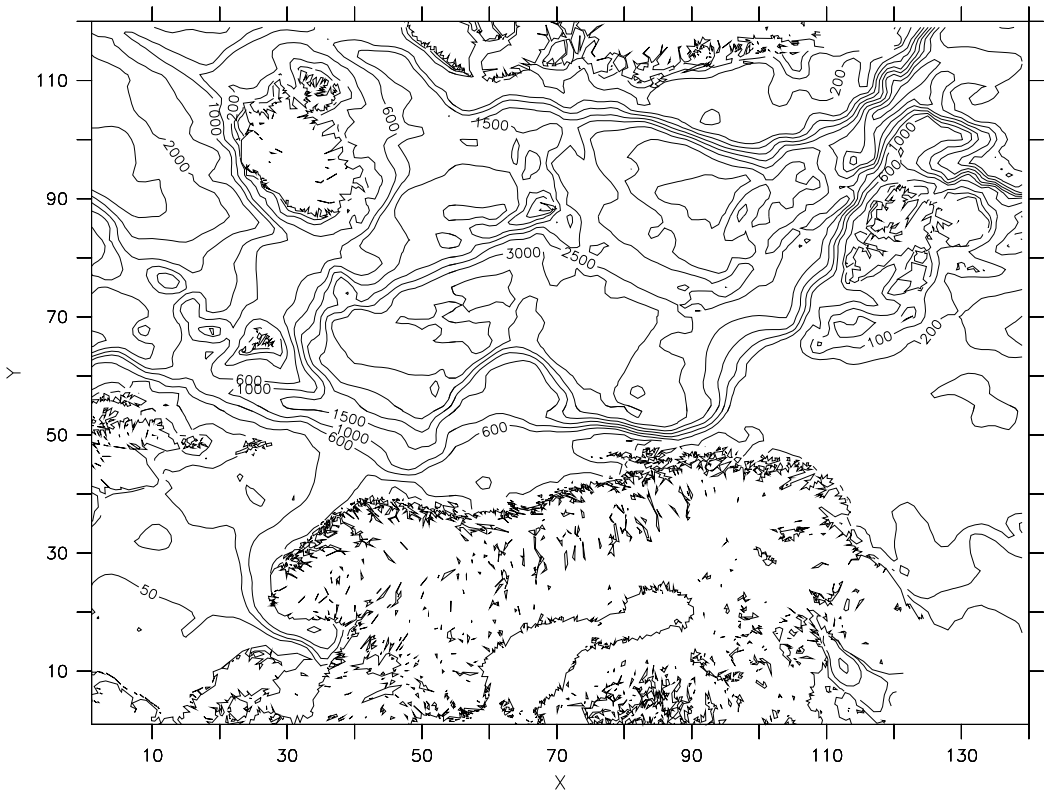

Figure 2: The bathymetry of the 20km resolution model.

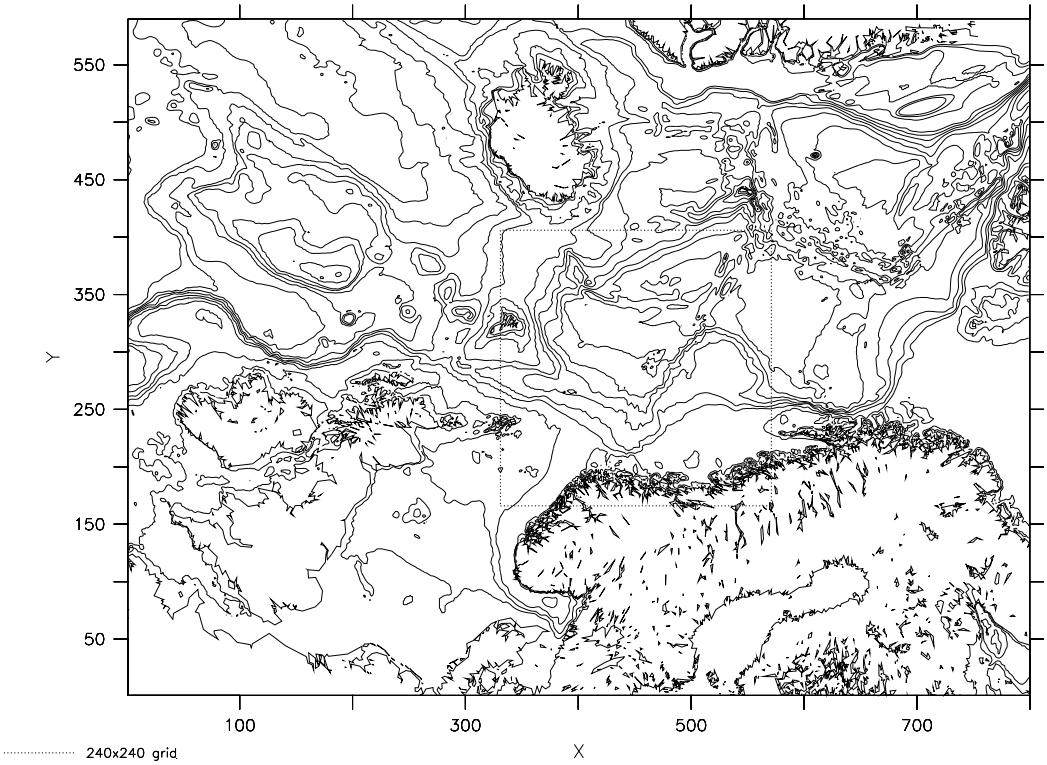

Figure 3: The bathymetry of the 4km resolution model using the same contour levels as in Figure 2. The model area for the 240x240 grid model outlined with a rectangle.

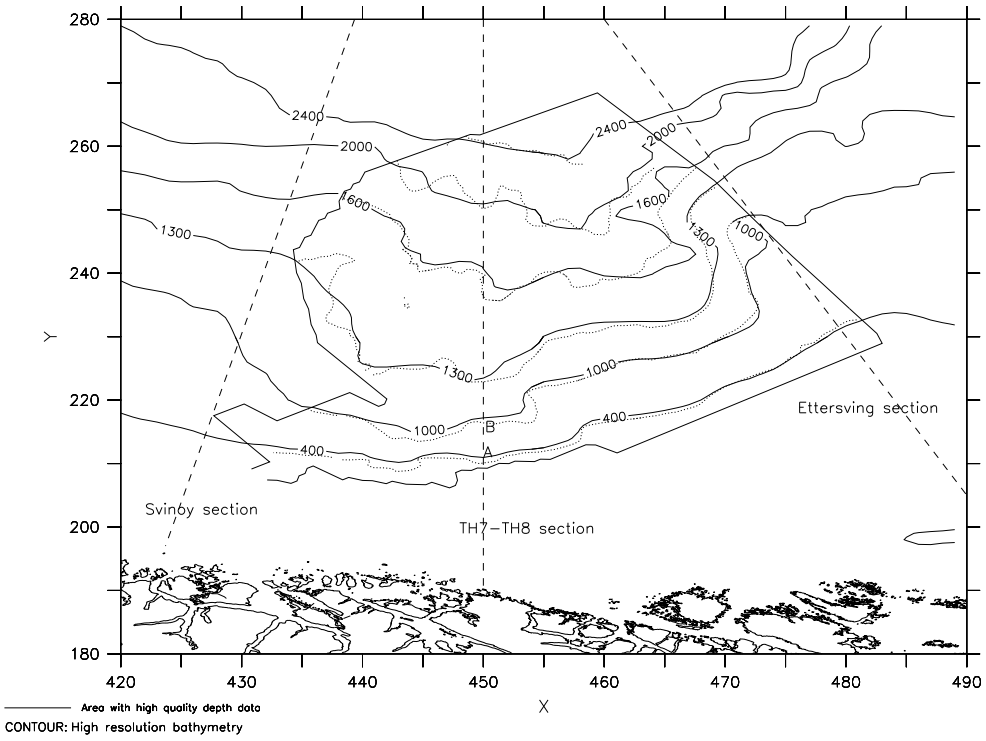

Figure 4: Dotted contours demonstrate new topographic features incorporated in the 800x590 4km resolution model, using the high resolution bathymetry data provided by Norsk Hydro. The approximate position of TH7 is marked A, TH8 is marked B.

December 2002 and January 2003. The stick vectors for wind above station TH7 are shown in Figure 5. We observe that the strength of the wind forcing peaks around mid January for station TH7. The effect of the forcing was turned on gradually over ca. 2000 time-steps using an exponential ramp function $f(t) = 1 - e^{-1\times10^{-5}t}$. Figure 6 shows a strong low

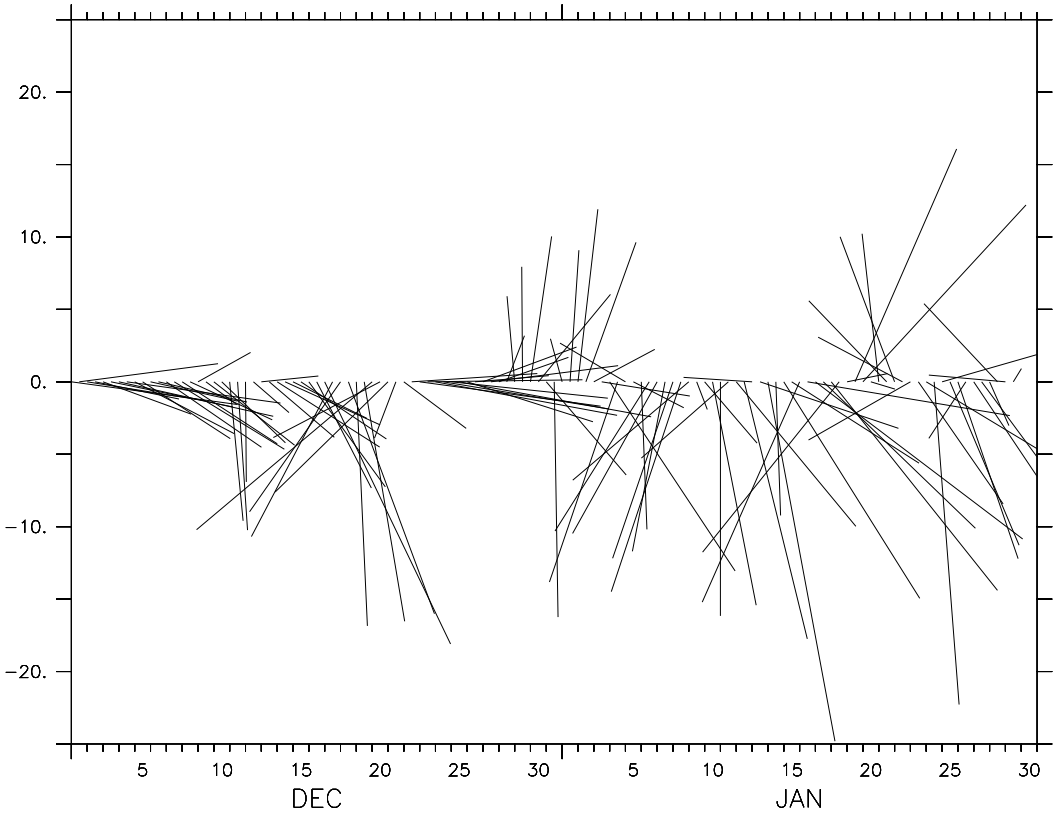

Figure 5: Wind speed over TH7, Y-axis shows magnitude (m/s), X-axis time in days.

pressure system south-west of Iceland, mid January 2003. It is the effect of such systems we want to examine by enlarging the model domain.

3 Results

3.1 Time series from station TH7 and TH8

Figures 8-9 shows the timeseries for speed at selected depths for the stations TH7 and TH8, obtained during the measurement program at OL. Comparing the timeseries with the diagram for wind forcing in Figure 5 we recognize that also the measured speed at all depths have a peak around day 45 of the selected period (mid January 2003). The speed has a high degree of variability, with a high frequency signal with period of minutes on top of slow changes with a period of days. In Figure 7 we show a direct comparison of the measured speed under TH7 and the large domain 4km model in the period from day 44 to 50. We observe that the model currently is stepped forward in time with a time step (approximately 4 minutes) that makes it impossible to capture the real life rapid changes in speed. The two signals are quite different, but in periods with strong dynamical behaviour we see a similar trend. Due to the resolution the model can capture wind driven events, but not events due to effects of internal pressure, such as eddies. This could explain what we see in Figure 7, some trends seem to be represented by the numerical model, others not at

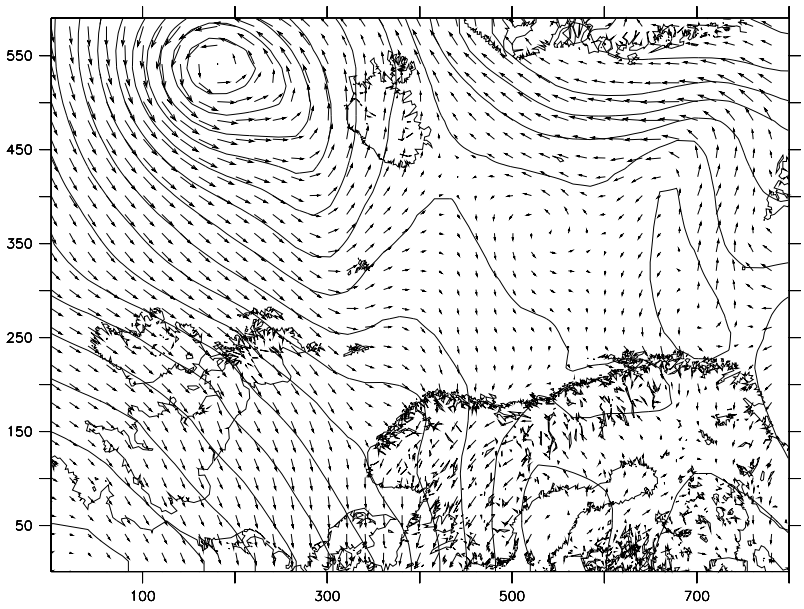

Figure 6: Wind and strong low pressure system south of Iceland, January 14th 2003.

all.

Figure 10 shows the time series of speed at 69 meter depth (left) and 269 meter depth (right) for the three 20km resolution runs at station TH7. We observe a high frequency oscillation with period of approximately 12 hours, inertia waves. We observe a peak in speed after approximately 45 days, that corresponds well with the forcing. We see a dramatic increase in amplitude for the oscillations when we reduce the horizontal viscosity by a factor of 5. The amplitude grows gradually from a modest start, and is stronger in the higher levels of the water column. When we reduce the thickness of the initial thermocline to approximately 20m, we observe the same large oscillations, but they appear earlier. This tells us that the oscillations may be strongly influenced by internal processes. We also know that we do not resolve such processes with 20km resolution. Compared to the measurements we only recognize the strong wind event around day 45.

Figure 11 and 12 shows the time series for speed at station TH8, but at the depths 113, 373, 533, and 738 meters. We see the same effects as for TH7 but not as clear. In Figure 13 we again see the time series for speed at station TH7, but for the reduced area 4km model. Compared to the 20km models, we see dramatic differences in the dynamics: the maximum speed rarely exceeds 30 cm/s, but we observe an oscillation with similar period to that of the 20 km resolution runs and with much smaller amplitude. We observe also in these series an increased activity between 45 and 50 days, which is consistent with the 20km run. We believe the main reasons for these results to be the reduced area - we miss the effects of processes taking place outside the domain. To get stable results, it was also necessary to use larger horizontal viscosities. Figure 14 shows time series for station TH8 plotted at the same 4 depths as the 20 km simulation. We observe that the time series are even more damped out at this station. Compared to the measurements, the magnitude of speed are generally too small, but the amplitutde of the high resolution signal has become more realistic.

Figures 16 and 17 show the time series from the last model run, where we increased the model domain to cover an area even larger than the 20km model, included new and improved numerics, reduced the horizontal viscosity, and reran the simulation with the same forcing and 4km resolution. Again dramatic differences. We still spot the period of the fast

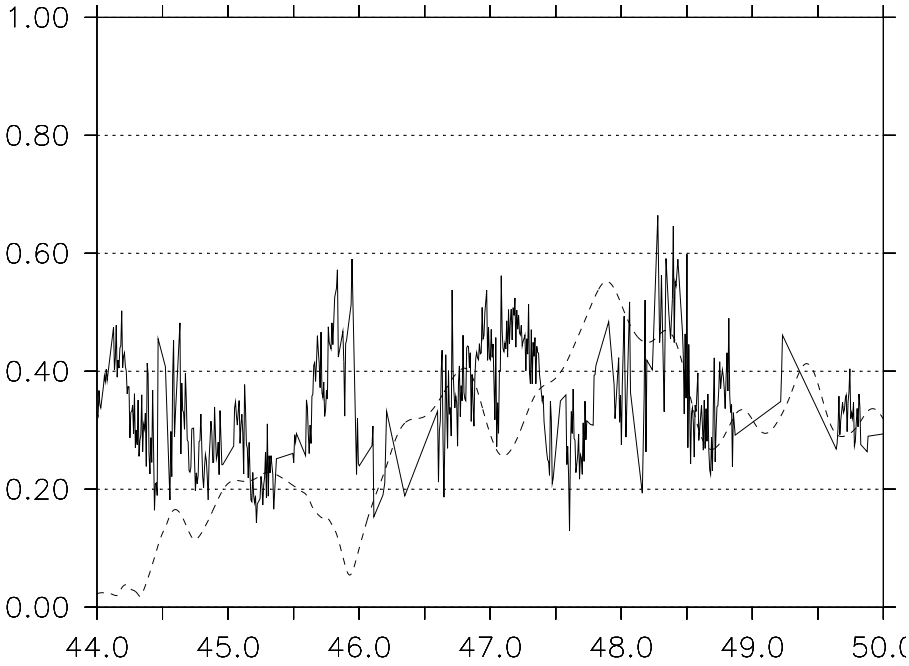

Figure 7: The solid line shows measured speed (m/s) at 72 m depth versus model (dashed line) at 69 m depth, near TH7, between day 44 and 50 of the simulation.

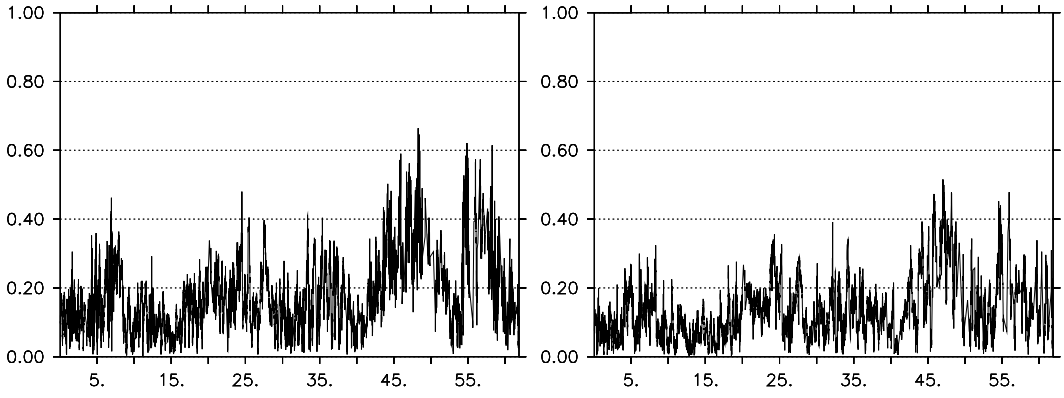

Figure 8: Measured speed (m/s) at 72 m depth (left) and 272 m depth (right) versus time in days at TH7.

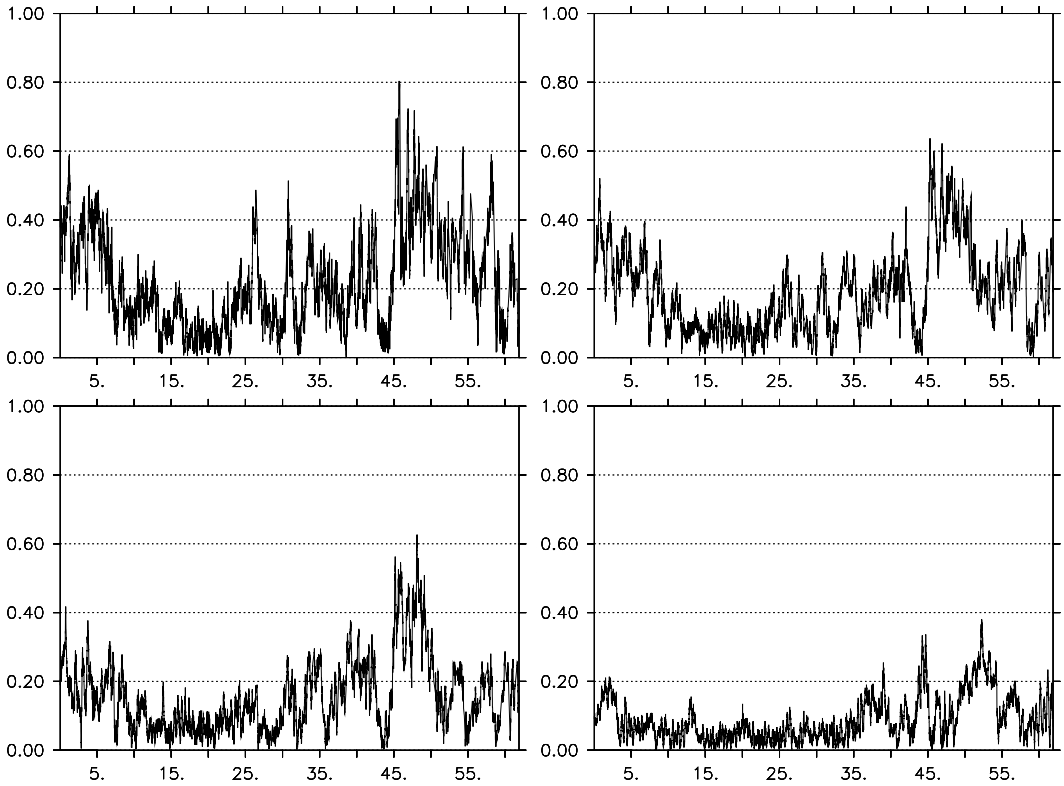

Figure 9: Measured speed (m/s) at 123m depth (top left), 383m depth (top right), 503m depth (bottom left), and 765m depth (bottom right) versus time in days at TH8.

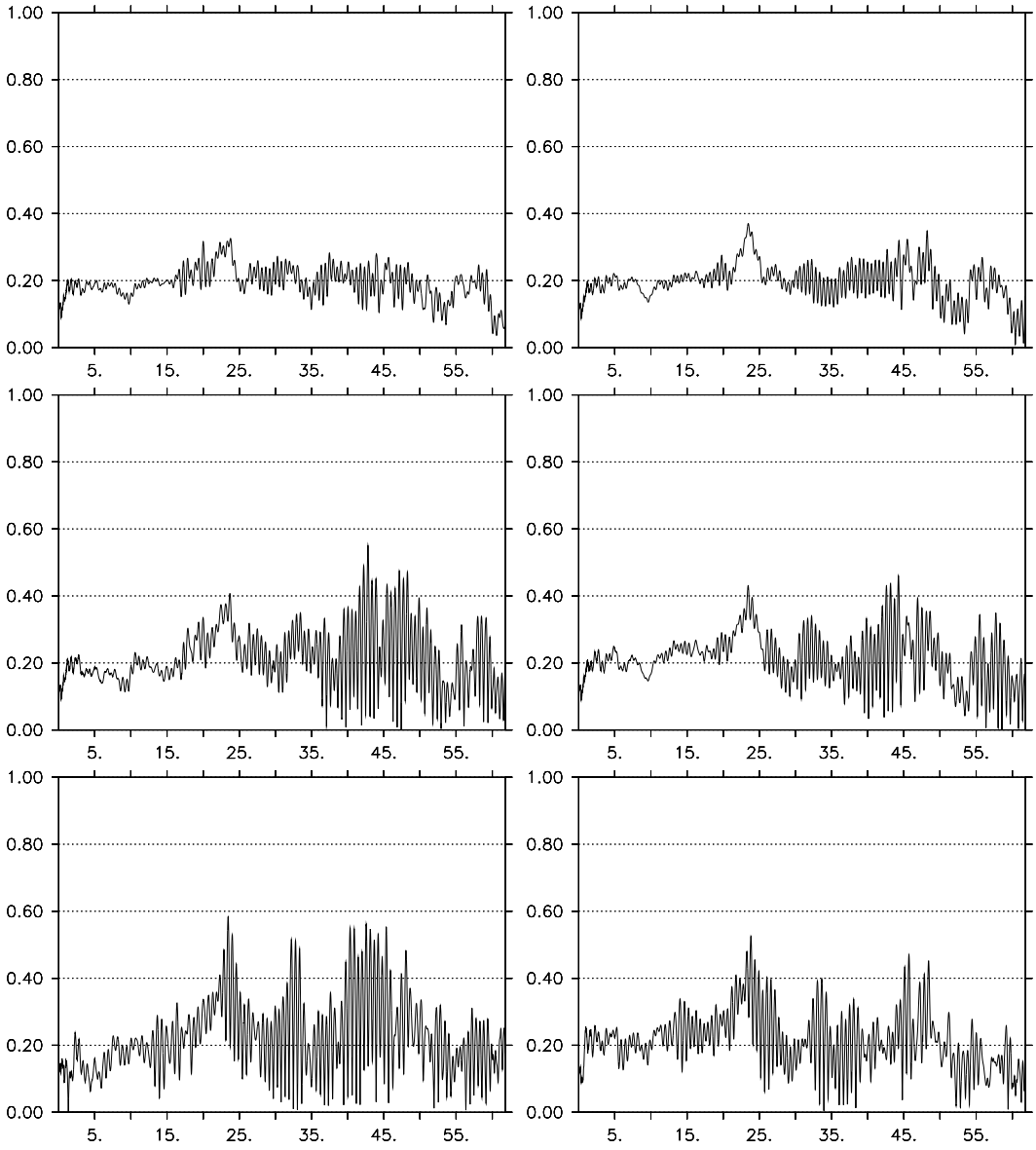

Figure 10: Speed (m/s) at 69 m depth (left) and 269 m depth (right) versus time in days at TH7 using the 20km model. The top row is from the run with $C_M = 0.5$ and the standard climatology initially. The middle row from the run with $C_M = 0.1$. The bottom row $C_M = 0.1$, and the initial climatology is modified so that the thermocline is only 20m thick.

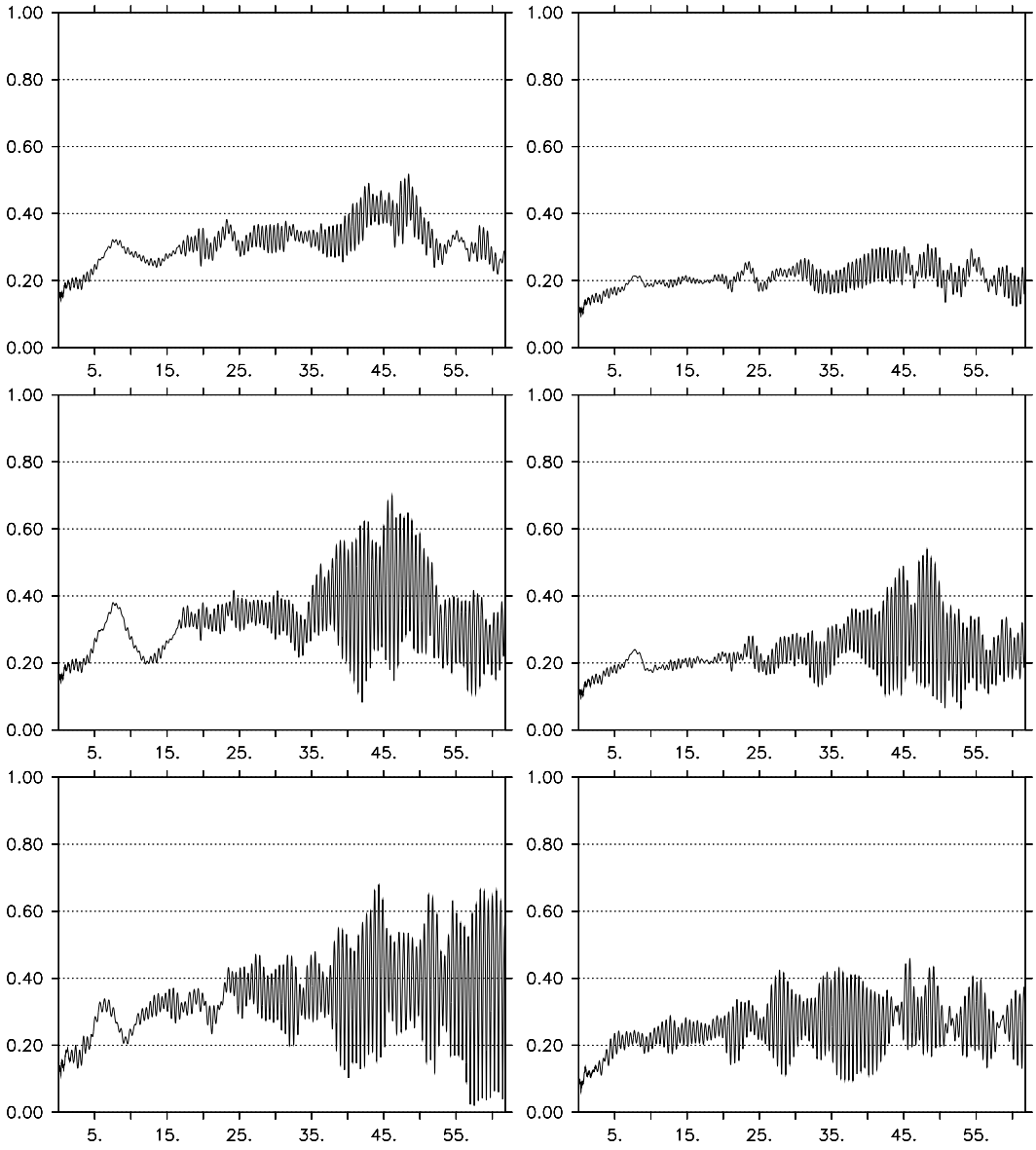

Figure 11: Speed (m/s) at 113 m depth (left) and 373 m depth (right) versus time in days at TH8 using the 20km model. The top row is from the run with $C_M = 0.5$ and the standard climatology initially. The middle row from the run with $C_M = 0.1$. The bottom row $C_M = 0.1$, and the initial climatology is modified so that the thermocline is only 20m thick.

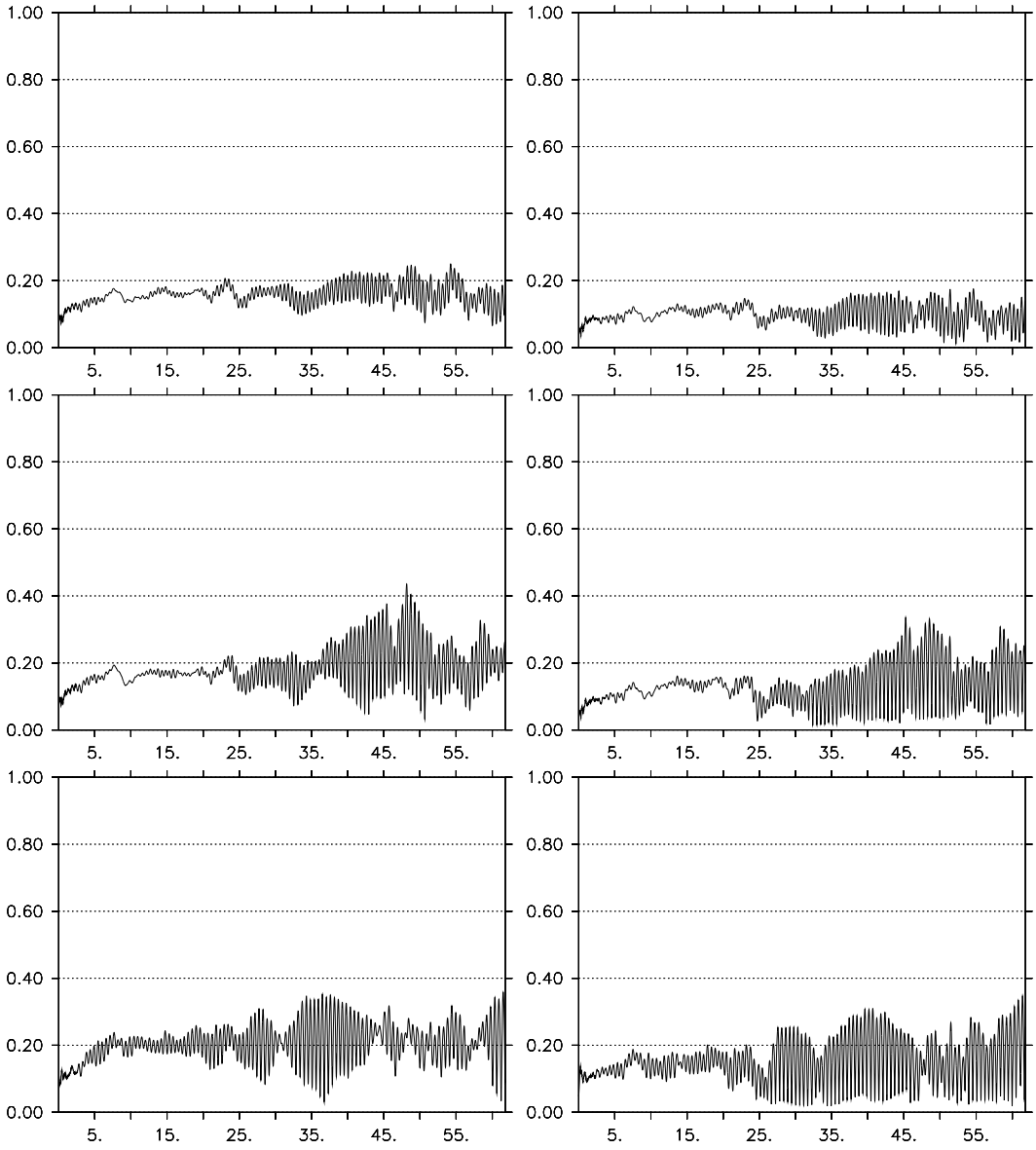

Figure 12: Speed (m/s) at 553 m depth (left) and 738 m depth (right) versus time in days at TH8 using the 20km model. The top row is from the run with $C_M = 0.5$ and the standard climatology initially. The middle row from the run with $C_M = 0.1$. The bottom row $C_M = 0.1$, and the initial climatology is modified so that the thermocline is only 20m thick.

inertial oscillations, with an amplitude similar to the reduced area 4km model. The longer timescale signal however, is different. We reach a maximum speed after approximately 45 days, consistent with the other simulations. The speed however, now reaches a magnitude of up to 70 cm/s. This result is in better agreement with the measurements, as is the amplitude of the high speed oscillation. If we compare the measurements with simulations from station TH7 from day 30 until the end, it is clear that the major trends are the same, two peaks in the maximum speed aorund day 45 and 55, and a period where the signal shows similar shape between day 27 and day 40. Since the model was started from a smooth climatology, any realism is not to be expected in the first half of the simulation. A very high velocity current of e.g. 20 cm per second would use 45 days to reach OL from the areas around Iceland. In the timeseries for temperature under TH8 in Figure 15 we see that the model thickness of the thermocline seems to stabilize after approximately 30 days.

The maximum simulated speed at TH8 is still smaller than observed, but from the results from the 20km model it is clear that with an even lower horizontal viscosity and a more realistic, reduced thickness thermocline, the dynamic response to the strong low pressure systems would be much stronger. We observe that the model results from TH7 generally correspond better to measurements than those from TH8. We believe the reason for this is that most of the TH8 stations are situated deeper than those of TH7. At larger depths baroclinic processes dominate, which the model, with 4km resolution cannot reproduce. One example of such a baroclinic event is the extreme increase in speed at day 45, when at e.g. 123m depth the speed goes up from near 0 to almost 80 cm/s. We spot the event in the time series for temperature 15, while the modelled series for speed at TH8 stations only shows a modest peak in that period.

We also experience the largest velocities in the middle of the water column, while measurements shows a decrease in maximum speed at increasing depth. One explanation for this can be that we still have not run the model long enough to get a realistic thermocline. Rerunning the experiment with lower viscosity would improve this situation, as the water masses would react quicker to the applied forcing.

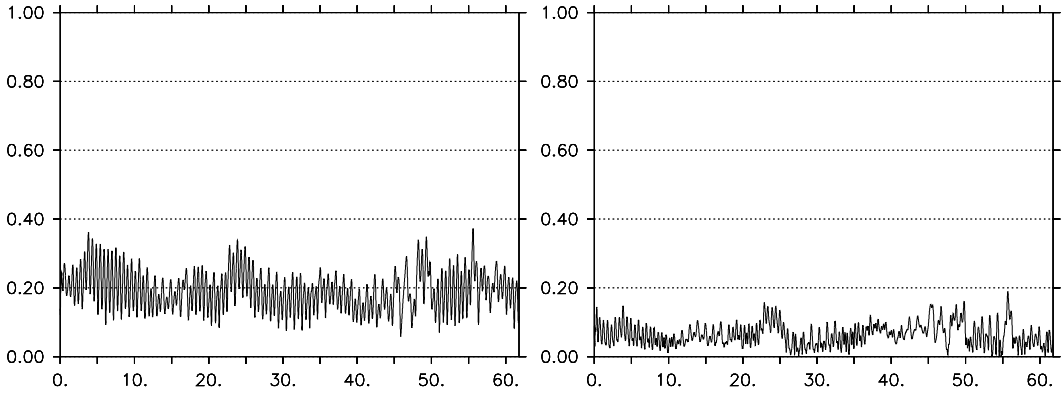

Figure 13: Speed (m/s) at 69 m depth (left) and 269 m depth (right) versus time in days at TH7 using the reduced area 240x240 4km model.

Figure 15 shows the time series of temperature in the water column below station TH8. We observe that the thickness of the thermocline decreases during the simulated period. This is as expected as we start from climatology. Realistic fields show even sharper gradients and far more variability.

We recognize the before mentioned event after approximately 45 days, as a strong dip in the temperature at a few hundred meters depth, most likely related to the strong atmospheric forcing experienced in the same period, see Figure 5. Such events have been observed and are mostly followed by a strong increase in flow velocity. In the time series for speed for the 4km full domain simulation, we observe a major peak in the velocity at TH7 just after

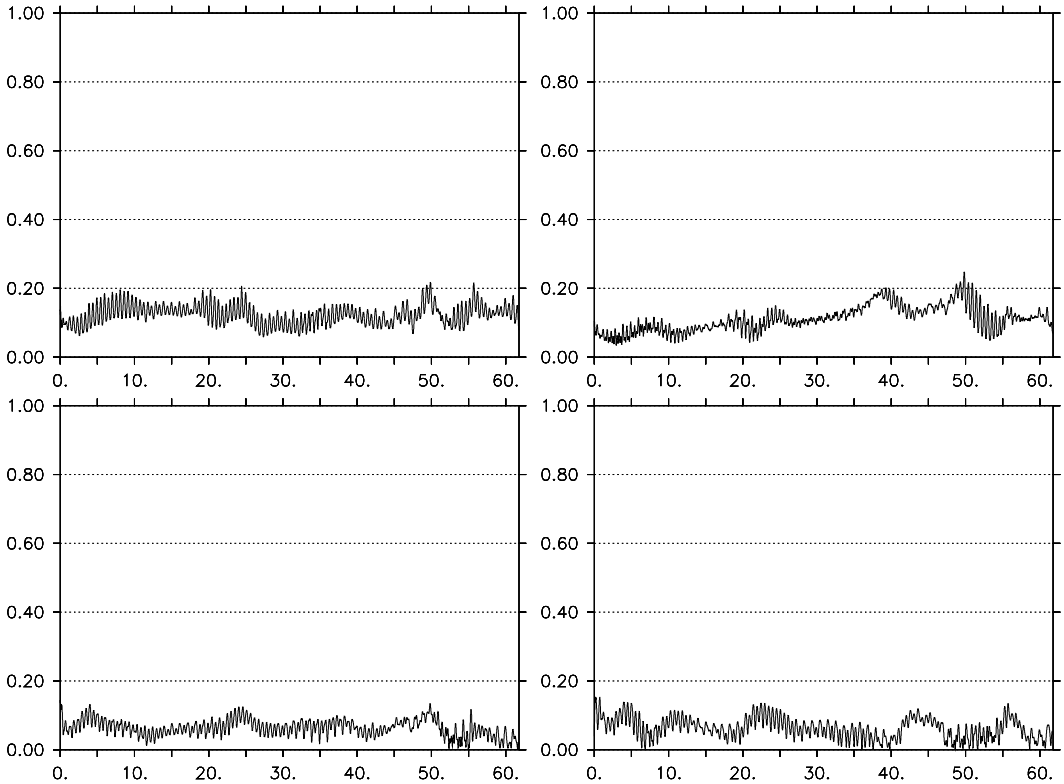

Figure 14: Speed (m/s) at 113m depth (top left), 373m depth (top right), 533m depth (bottom left), and 738m depth (bottom right) versus time in days at TH8 using the reduced area 240x240 4km model.

45 days, but we also see that the model response is much slower than the measured time series.

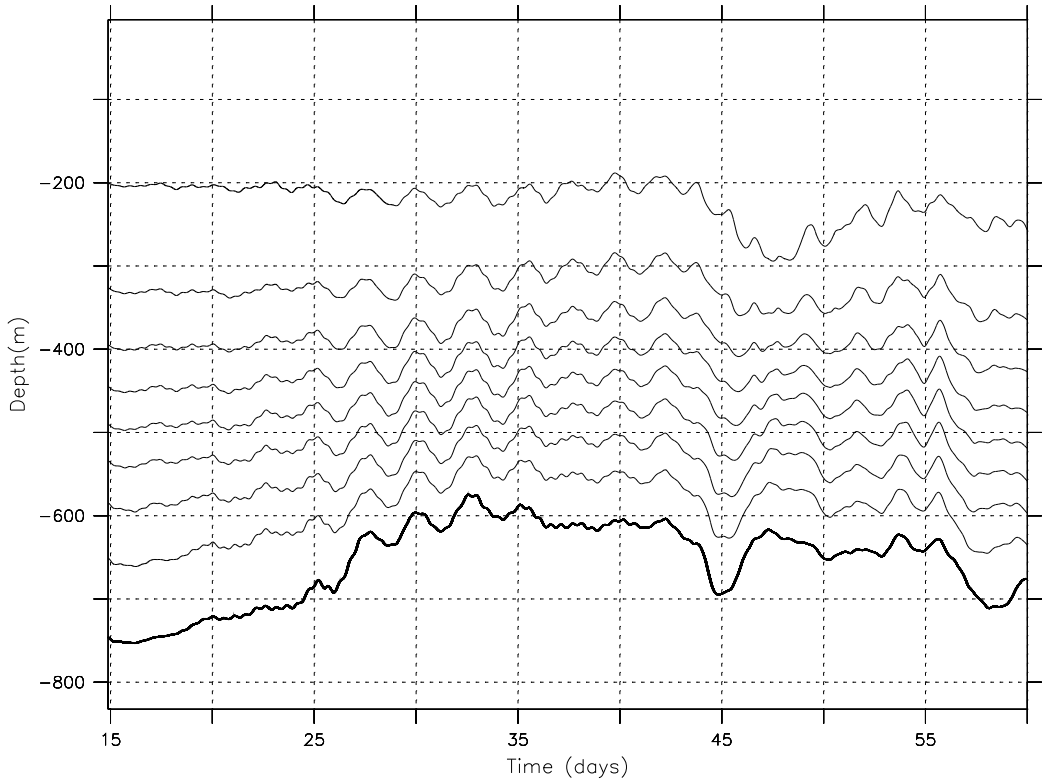

Figure 15: Time series of temperature at TH8, bottom thick line 0°, one degree intervals up-wards.

3.2 Water masses initially, just before and after the main event at OL, in the full extent 4km resolution study

Figures 18-20 show the salinity through the three subsections shown in Figure 4 in the Ormen Lange area. The climatological salinity distributions in all cross sections are very smooth initially, and we observe how the water masses during the simulation become almost fully vertically mixed on the relatively shallow shelf. This is consistent with measurements from a typical winter.

We observe a core of salty (Salinity > 35.1) atlantic water which is relatively stable in position. Close to the shelf edge, we observe that the contour lines for less salty water are lifted up on the shelf during the wind event that peaks after ca 45 days. We also see that these water masses starts to sink after the event. The 0 degree isotherm is, near the shelf edge, lifted from a level of approximately -750 meters up to ca. -590 meters in the cross section through TH7 and TH8 as can be seen in Figure 19.

We observe that the horisontal extent of the run-up is relatively thin, and that the water masses further away from the shelf seem to be little affected. This is consistent with the prediction of Martin Mork [12].

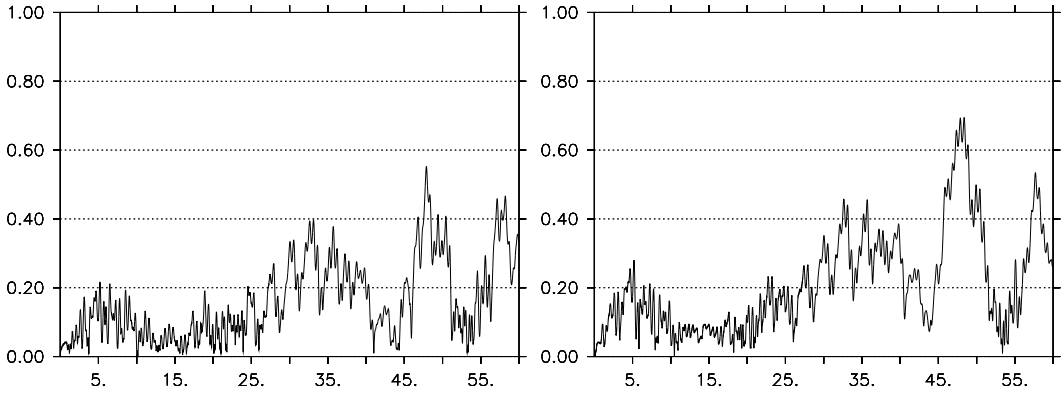

Figure 16: Speed (m/s) at 69 m depth (left) and 269 m depth (right) versus time in days at TH7.

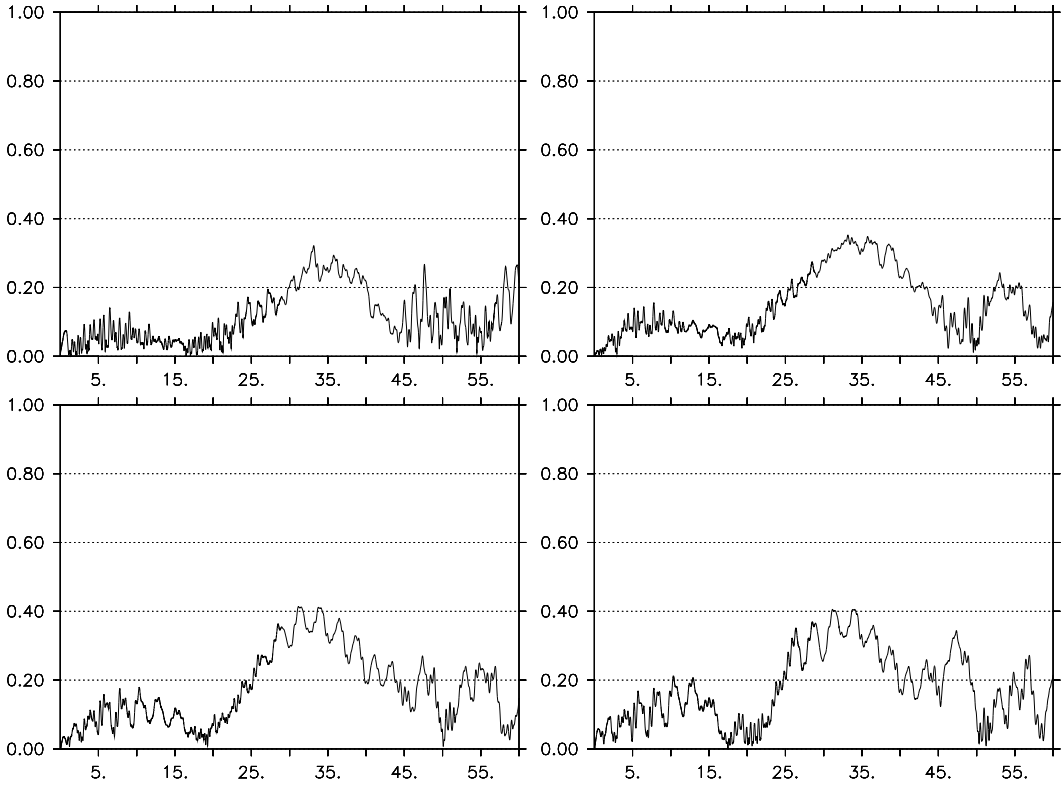

Figure 17: Speed (m/s) at 113m depth (top left), 373m depth (top right), 533m depth (bottom left), and 738m depth (bottom right) versus time in days at TH8.

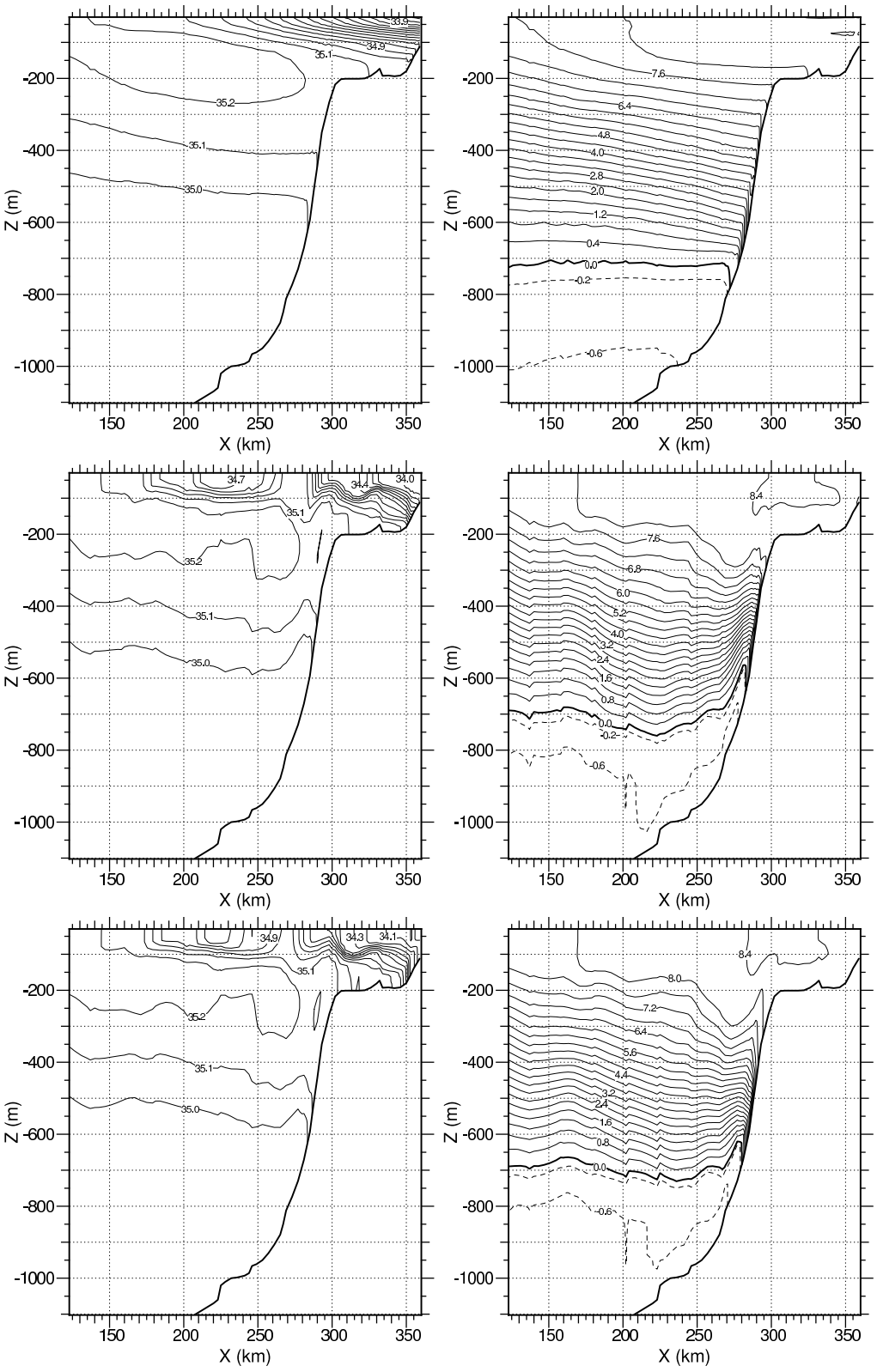

Figure 18: The Salinity (left) and Temperature (right) in the Svinoy section after 0, 46 and 48 days.

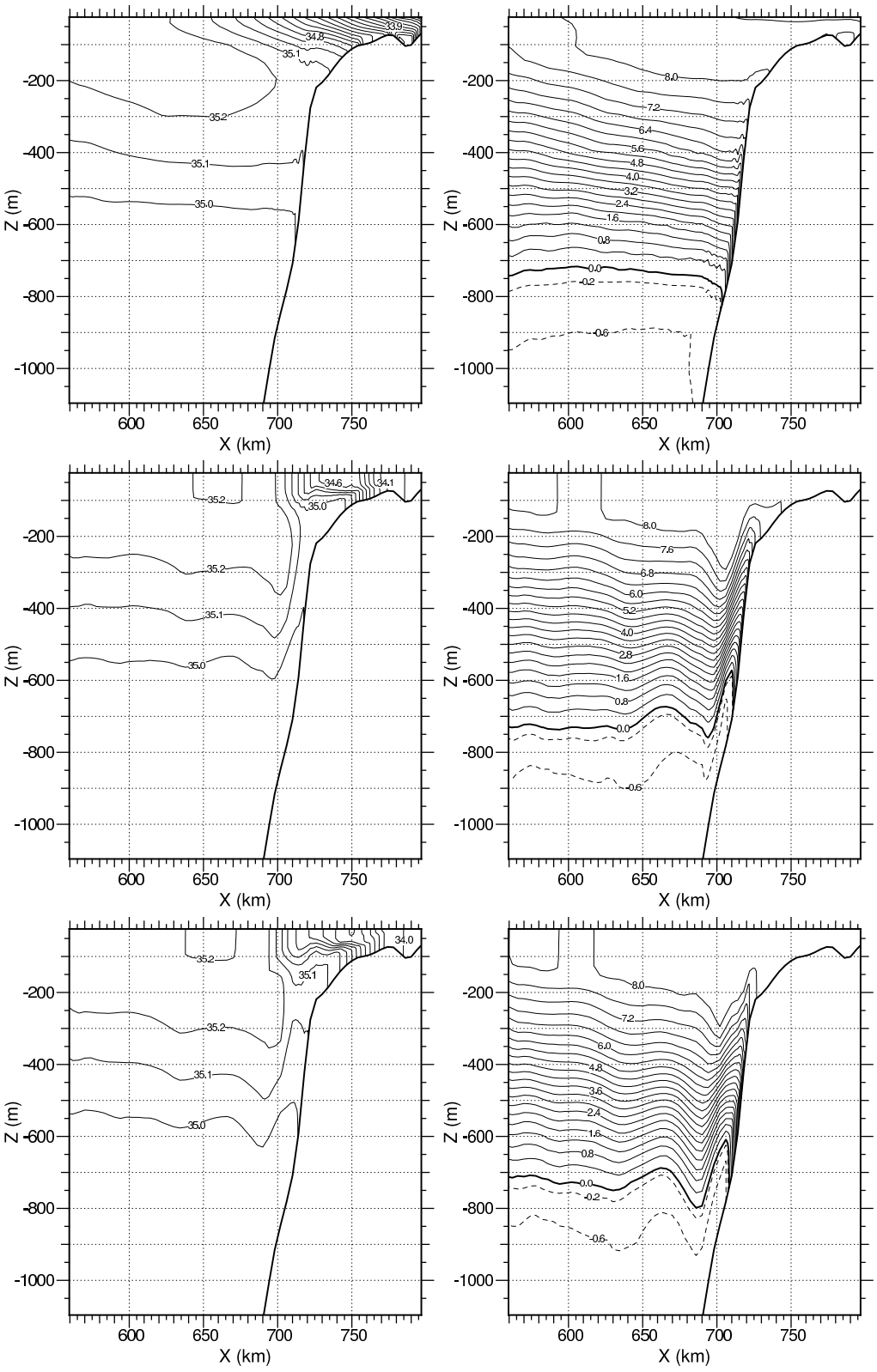

Figure 19: The Salinity (left) and Temperature (right) in the section through TH7(at ca. 400m depth) and TH8(at ca. 800m depth) after 0, 46 and 48 days.

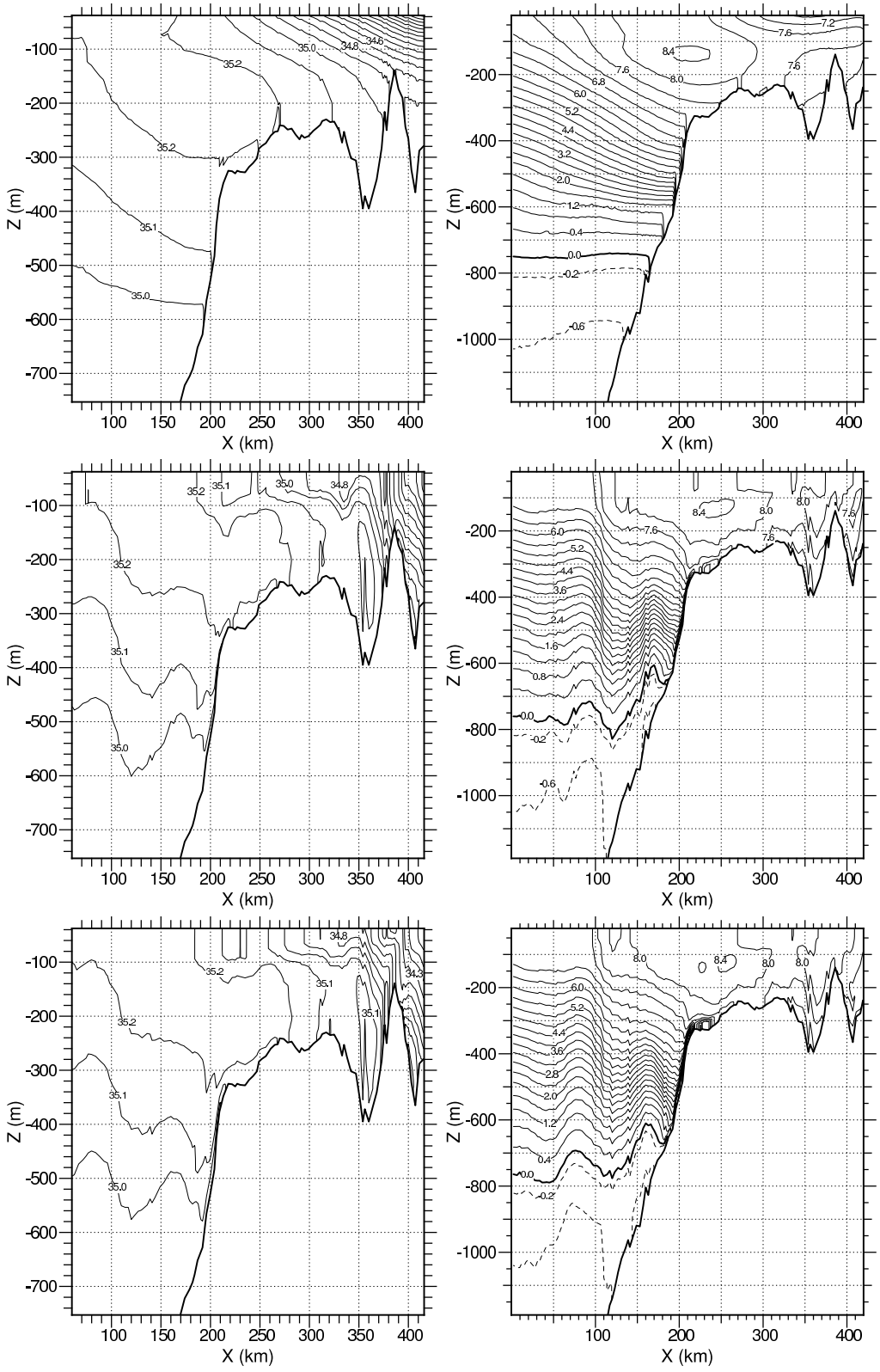

Figure 20: The Salinity (left) and Temperature (right) in the “Ettersving”-section after 0, 46 and 48 days.

4 Conclusions

In this report, we have presented some results from the Ormen Lange area from simulations of the Norwegian Seas using 4 and 20 km resolution, and 3 different geographical extents.

The initial simulations using 4 km resolution and a reduced area gave too small dynamic response to the relatively strong low pressure system activity in the given period. The 20km resolution results showed that by reducing the viscosity and enlarging the simulation domain, a much stronger response could be obtained. The response was further strengthened by starting from an initial climatology with a thinner thermocline. A more recent version of BOM was then set up for a much larger domain and with relatively high resolution (4km) - covering the most relevant parts of the atlantic inflow. It was demonstrated that even when starting from a smooth initial climatology, this model can produce results that are in far better agreement with measurements. The results from the simulations using 20 km resolution demonstrate that the 4km results can be further improved upon by reducing the horizontal viscosity and starting the simulation with a more realistic thermocline.

The large extent 4 km model is compututationally too expensive to be used for routine studies. This is partly due to lack of speed of available HPC resources, but also due to limitations with the current parallelization of the model. The parallelization technique (shared memory OpenMP directives) is simple to implement and has required small changes to the code, but it does not scale well for large problems. The solution to the scalability problem is to introduce message passing parallelism into the code (e.g. MPI), which also enables the use of the code on currently popular Linux clusters.

Acknowledgements

This work has been supported by Norsk Hydro under contract number 5259646.

The author(s) wish to acknowledge the use of the Ferret program for analysis and graphics in this report. Ferret is a product of NOAA's Pacific Marine Environmental Laboratory. (Information is available at http://www.ferret.noaa.gov)

References

[1] J. Berntsen. Users guide for a modesplit σ-coordinate numerical ocean model. version 1.0. Technical Report 135, Department of Applied Mathematics, University of Bergen, 2000.

[2] T. Eldevik, I.K. Eliassen, J. Berntsen, and G. Furnes. On the influence of the thermohaline circulation at Ormen Lange. Technical report, Bergen, May 2001.

[3] I.K. Eliassen. A numerical simulation of the local response of currents at Ormen Lange to a travelling storm. Technical Report CMR-01-A50005, Christian Michelsen Research, Bergen, 2001.

[4] I.K. Eliassen and J. Berntsen. Using a σ-coordinate numerical ocean model for simulating the circulation at Ormen Lange. Technical Report 138, Department of Mathematics, University of Bergen, January 2000.

[5] I.K. Eliassen, T. Eldevik, J. Berntsen, and G. Furnes. The current conditions at Ormen Lange - Storegga. November 2000.

[6] H. Engedahl, B. Ådlandsvik, and E. Martinsen. Production of monthly mean climatological archives of salinity, temperature, current and sea level for the nordic seas. *Journal of Marine Systems*, 14:1–26, 1998.

[7] B. Galperin, L.H. Kantha, S. Hassid, and A. Rosati. A quasi-equilibrium turbulent energy model for geophysical flows. *J. Atmos. Sci.*, 45:55–62, 1988.

[8] A.E. Gill. *Atmosphere-Ocean Dynamics*. Academic Press, 1982. ISBN-0-12-283520-4.

[9] D.R. Lynch, J.T.C. Ip, C.E. Naimie, and F.E. Werner. Convergence studies of tidally-rectified circulation on Georges Bank. In American Geophysical Union, editor, *Quantitative Skill Assessment for Coastal Ocean Models*. American Geophysical Union, 1994.

[10] E.A. Martinsen and H. Engedahl. Implementation and testing of a lateral boundary scheme as an open boundary condition in a barotropic ocean model. *Coastal Engineering*, 11:603–627, 1987.

[11] G.L. Mellor and T. Yamada. Development of a turbulence closure model for geophysical fluid problems. *Rev. Geophys. Space Phys.*, 20:851–875, 1982.

[12] M. Mork. On oceanic responses to atmospheric forces. In A.J. Lee and H. Charnock, editors, *Physical Variability in the North Atlantic - Proceedings of a Symposium held in Dublin, 25-27 September 1969*, pages 184–190. International Council of the Exploration of the Sea, 1972.

[13] J. Smagorinsky. General circulation experiments with the primitive equations, I. The basic experiment. *Mon. Weather Rev.*, 91:99–164, 1963.

[14] F. Vikebø, J. Berntsen, and G. Furnes. Numerical studies of the current response at Ormen Lange to a travelling storm. Technical Report 162, Department of Mathematics, University of Bergen, 2001.

[15] F. Vikebø, J. Berntsen, and G. Furnes. Numerical studies of the response of currents at Ormen Lange to travelling storms. *Journal of Marine Systems*, 45:205–220, 2004.

[16] H.Q. Yang and A.J. Przekwas. A comparative study of advanced shock-capturing schemes applied to Burgers equation. *J.Comp.Phys.*, 102:139–159, 1992.